

**Scattering of elastic waves by a periodic monolayer of spheres**

R. Sainidou and N. Stefanou

*University of Athens, Section of Solid State Physics, Panepistimioupolis, GR-157 84 Athens, Greece*

I. E. Psarobas\* and A. Modinos

*Department of Physics, National Technical University of Athens, Zografou Campus, GR-157 80 Athens, Greece*

(Received 4 February 2002; published 8 July 2002)

Using the multiple-scattering formalism we developed in a previous work, and extended here, we analyze available experimental data on the transmission of longitudinal waves in the system: water-slab of polyester-water, the slab of polyester having a plane of glass or lead or steel spheres in the middle. The theoretical results reproduce accurately the measured spectra and provide a transparent physical picture of the underlying processes. In particular, the dips in the observed spectra are attributed to multiple wave scattering between the spheres, and are related to hybridization-induced gaps in the frequency band structure of the longitudinal elastic modes of a corresponding infinite crystal.

DOI: 10.1103/PhysRevB.66.024303

PACS number(s): 46.40.-f, 43.40.+s, 43.20.+g

**I. INTRODUCTION**

The propagation of elastic waves in inhomogeneous media has attracted a lot of attention over the years as it relates to many and varied disciplines ranging from geophysics to mechanical engineering, and to diverse applications such as the quantitative nondestructive evaluation, the design of ultrasound absorptive materials, etc. More recently there has been growing interest in a special type of inhomogeneous materials, the so-called phononic crystals: the elastic constants vary periodically in space. It has been pointed out that in such systems the possibility exists of absolute spectral gaps, i.e., regions of frequency over which elastic waves cannot propagate in the material, which in turn promises interesting applications such as nonabsorbing mirrors and vibration-free cavities. Phononic crystals are also interesting from a basic physics point of view, for example, in relation to Anderson localization of classical waves: one expects that the introduction of a certain amount of disorder will lead to the localization of the vibrational modes near the edges of a spectral gap. Numerous studies of phononic crystals in one, two, and three dimensions have been reported in the last few years (see, e.g., Ref. 1, and references therein). However, the intermediate structure, an elastic matrix containing a single layer of inclusions, has received considerably less attention.

We have developed a formalism for the calculation of the frequency band structure of phononic crystals consisting of nonoverlapping spheres in a host medium of different elastic constants.<sup>2</sup> The formalism allows one to also calculate the transmission, reflection, and absorption coefficients of an elastic plane wave incident, at any angle, on a slab of the material and, therefore, it can describe the physical situation in an actual transmission experiment. The slab may consist of a single plane of spheres [a two-dimensional (2D) periodic array of spheres corresponding to a given crystallographic plane] or a stack of such planes. We have already applied the method to some cases of practical interest.<sup>3-5</sup> In this paper we use it to study the transmission of elastic waves through periodic monolayers of spheres. We compare our results with

relevant experimental data and provide a consistent interpretation of the transmission spectra of these systems.

**II. ELASTODYNAMIC RESPONSE OF A PLANE OF SPHERES**

The present paper is motivated to a large degree by some recent work of Kinra and co-workers<sup>6-9</sup> concerning the scattering of elastic waves by a plane of nonoverlapping spheres of radius  $S$ , centered on the sites of a 2D lattice. The plane of spheres is placed in the middle of a solid slab of polyester ( $\rho = 1220$  kg/m<sup>3</sup>,  $c_l = 2490$  m/sec,  $c_t = 1180$  m/sec), 7 cm thick, which is immersed in water ( $\rho_w = 1000$  kg/m<sup>3</sup>,  $c_{wl} = 1480$  m/sec,  $c_{wt} = 0$ ). The spheres themselves are made of glass ( $\rho_s = 2490$  kg/m<sup>3</sup>,  $c_{sl} = 5660$  m/sec,  $c_{st} = 3300$  m/sec), lead ( $\rho_s = 11300$  kg/m<sup>3</sup>,  $c_{sl} = 2210$  m/sec,  $c_{st} = 860$  m/sec), or steel ( $\rho_s = 7800$  kg/m<sup>3</sup>,  $c_{sl} = 5940$  m/sec,  $c_{st} = 3200$  m/sec). Absorption is not negligible in polyester ( $\alpha_l = 0.17$  nepers/cm at 1 MHz,  $\alpha_t = 0.35$  nepers/cm at 1 MHz) and in lead ( $\alpha_{sl} = 0.13$  nepers/cm at 1 MHz); this is taken into account in our calculations unless otherwise stated. An elastic wave in water (only longitudinal waves exist in water) of given angular frequency  $\omega$  is incident normally on the polyester slab containing the plane of spheres, and is partly reflected, partly transmitted and partly absorbed by it. The corresponding transmittance defined, as usual, as the ratio of transmitted over incident flux of energy, is denoted by  $T$ . Similarly a wave in water, of the same frequency, incident normally on the slab of polyester when there are no spheres of any kind in it, will be partly transmitted, reflected and absorbed by it. We denote the corresponding transmittance by  $T_0$ , and refer to the ratio  $T/T_0$  as the normalized transmittance, which is the quantity measured in the experiments.<sup>6-9</sup> Typical experimental results are shown in Fig. 1, by the squares, for glass, lead, and steel spheres. In all cases, the spheres are centered on a square lattice of lattice constant  $a_0$ ; therefore a larger lattice constant corresponds to a lower coverage by the spheres. Similar results were obtained for a hexagonal lattice as for

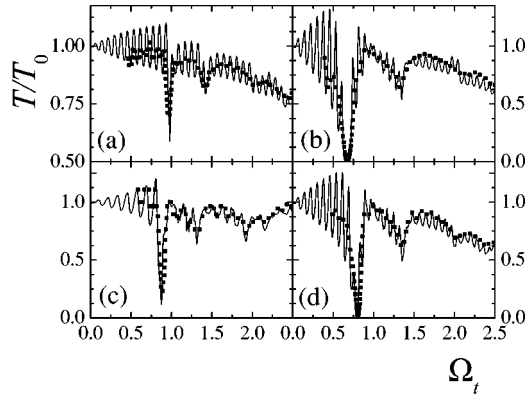


FIG. 1. Normalized transmittance for a longitudinal elastic wave incident normally on a square lattice of (a) glass spheres ( $S=0.56$  mm,  $a_0=2.63$  mm), (b) lead spheres ( $S=0.60$  mm,  $a_0=2.63$  mm), (c) steel spheres ( $S=0.585$  mm,  $a_0=3.95$  mm), (d) steel spheres ( $S=0.585$  mm,  $a_0=2.63$  mm), in the middle of a polyester slab, 7 cm thick, immersed in water. The theoretical results are shown by the solid lines and the experimental data by the squares.

the square one. The most striking feature of the experimental curves is the pronounced dip below  $\Omega_t = \omega a_0 / (2\pi c_t) = 1$ . This dip is deeper for the lead and steel spheres compared to the glass spheres, and becomes more pronounced by increasing the coverage. There are also some additional dips, shallower, at higher frequencies. The solid curves in Fig. 1 are theoretical curves obtained using our formalism.<sup>2</sup> This formalism takes fully into account the multiple scattering of the elastic wave by the 2D array of spheres. However, in Ref. 2 it was assumed that the host medium (polyester in the present case) extends to infinity on either side of the plane of spheres. In the experiments<sup>6-9</sup> the slab of polyester containing the spheres is immersed, as we have already stated, in water, and therefore the formalism of Ref. 2 needs to be extended to take into account the scattering of the elastic wave at the two polyester-water interfaces. The way to do this is summarized in the Appendix. As can be seen from Fig. 1 our theoretical results are in very good agreement with the experimental data.

We note in passing that the extended formalism now in place can be used to study other problems of interest, e.g., to the acoustic microscopy of liquid-loaded surfaces of periodic structures.<sup>10</sup> Multiple reflections between the slab-water interfaces lead to the periodiclike oscillations, so obvious in the theoretical curves. The period of these oscillations, known as Fabry-Perot-type oscillations, is inversely proportional to the thickness of the polyester slab, and it is practically the same in  $T_0$  for the homogeneous polyester slab and in  $T$  for the one containing the spheres. These oscillations survive very well in the theoretical normalized transmittance  $T/T_0$ , but they do not show so clearly in the experimental curves of Fig. 1, because of the spectral resolution of the experiments.<sup>6-9</sup>

We now turn our attention to the dips in the normalized transmittance shown in Fig. 1, which are so nicely reproduced by the theory. They are of course due to the multiple scattering of the elastic wave by the plane of spheres. Maslov

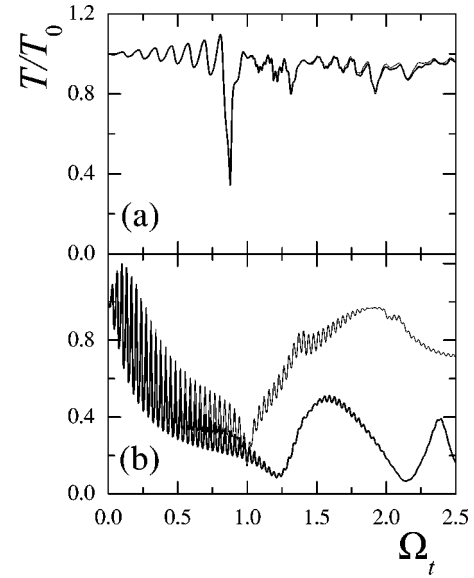


FIG. 2. Normalized transmittance for a longitudinal elastic wave incident normally on a square lattice [(a)  $a_0=3.95$  mm ( $A_f=0.07$ ), (b)  $a_0=1.17$  mm ( $A_f=0.79$ )] of steel spheres of radius  $S=0.585$  mm in the middle of a polyester slab, 7 cm thick, immersed in water, calculated using  $l_{\max}=1$  (thin lines) and  $l_{\max}=6$  (thick lines).

*et al.*<sup>9</sup> presented an approximate theoretical treatment of multiple scattering, assuming that spherical waves with  $l > 1$  do not scatter significantly by any single sphere of the plane of spheres. This, and to a lesser degree other approximations in their approach concerning the determination of the total incident wave on a given sphere, means that their treatment breaks down, as they themselves point out, when the coverage by the spheres  $A_f = \pi S^2 / a_0^2$ , exceeds a certain value. In terms of the formalism of Ref. 2, their treatment amounts essentially to keeping only terms with  $l \leq 1$  in the spherical-wave expansions of the elastic field. The inadequacy of this approximation is demonstrated in Fig. 2 which shows the normalized transmittance for two cases, one of relatively low coverage ( $A_f=0.07$ ), where convergence is obtained within the above approximation; and one of high coverage ( $A_f=0.79$ , which corresponds to touching spheres), where one needs to keep terms up to and including  $l_{\max}=6$  to obtain convergence. We should say, however, that for a qualitative understanding of the physics involved in the present case, the scattering of  $l=1$  waves is sufficient, and this is because the scattering of longitudinal and transverse waves by a glass, lead, or steel sphere in polyester, is dominated by  $l=1$  waves over the considered frequency range.

It has been suggested<sup>7-9</sup> that the abovementioned dips in the transmittance are somehow related to the so-called Wood anomalies,<sup>11</sup> which in turn relate to threshold frequencies which arise as follows. The elastic field outside the spheres (in polyester) can be written as a sum of plane waves with wave vectors<sup>2</sup>

$$\mathbf{K}_{g\nu}^{\pm} = \mathbf{k}_{\parallel} + \mathbf{g} \pm [q_{\nu}^2 - (\mathbf{k}_{\parallel} + \mathbf{g})^2]^{1/2} \hat{\mathbf{e}}_z, \quad (1)$$

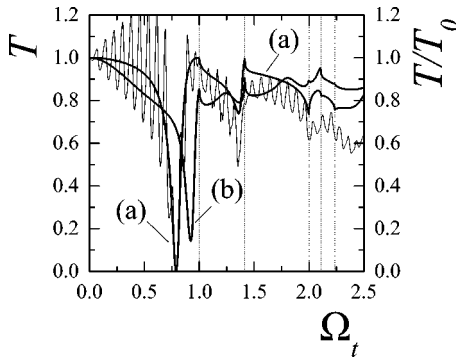


FIG. 3. Transmittance for a longitudinal [thick line (a)] and a transverse [thick line (b)] elastic wave incident normally on a square lattice ( $a_0 = 2.63$  mm) of steel spheres ( $S = 0.585$  mm) embedded in an infinite, nonabsorbing polyester matrix. The different vertical lines on the abscissa show the threshold frequencies for which  $q_\nu = |\mathbf{g}|$  for sets of  $\mathbf{g}$  vectors of increasing magnitude;  $\nu = l, t$ . The thin line refers to the normalized transmittance ( $T/T_0$ ) and is the same as in Fig. 1(d).

where  $\mathbf{k}_\parallel$  is a reduced wave vector within the surface Brillouin zone corresponding to the plane of spheres ( $xy$  plane),  $\mathbf{g}$  are the 2D reciprocal vectors corresponding to the given lattice, and  $\hat{\mathbf{e}}_z$  is the unit vector normal to the plane of spheres;  $q_\nu = q_l = \omega/c_l$  for a longitudinal wave and  $q_\nu = q_t = \omega/c_t$  for a transverse wave. Our calculations are done for  $\mathbf{k}_\parallel = \mathbf{0}$ , which relates to normal incidence. In this case, a set of  $\mathbf{g}$  vectors of the same magnitude  $|\mathbf{g}| > q_\nu$  define a corresponding set of evanescent waves, which means that the contribution of these beams to the elastic field decays exponentially with the distance from the plane of the spheres. As  $\omega$ , and therefore  $q_\nu$ , increases, we reach a threshold frequency above which this set of beams become propagating ( $|\mathbf{g}| < q_\nu$ ). One expects<sup>12</sup> and finds some structure in the transmittance associated with these threshold frequencies (Wood anomalies) as shown in Fig. 3. We note, however, that to obtain the thick curves of this figure, we have assumed that the medium (polyester) in which the plane of spheres is embedded extends to infinity on either side of this plane and that it is *not* absorbing. In this case (unlike in the experiments of Refs. 6–9) the incident wave may be longitudinal or transverse. The abovementioned threshold frequencies are indicated by the vertical lines in Fig. 3; one, at  $\Omega_t = 2.11$ , refers to a longitudinal beam, all the rest refer to transverse beams. It is evident that the minor structure associated with the above threshold frequencies is different in nature from the considerable dips in the transmission spectrum below  $\Omega_t = 1$  and from the shallower dips at higher frequencies; when absorption is taken into account, any minor structure associated with Wood anomalies is smoothed out to a very large degree (see Fig. 3).

In Fig. 3 we show also, by the thin line, our results for the actual experimental setup: a layer of steel spheres in the middle of a polyester slab immersed in water [the same as in Fig. 1(d)]. Comparison of the thick line (a) with the thin line of Fig. 3 shows that the main dip at  $\Omega_t = 0.79$  is not connected with or affected in any way by multiple reflections at the polyester-water interfaces or by absorption. Therefore, in

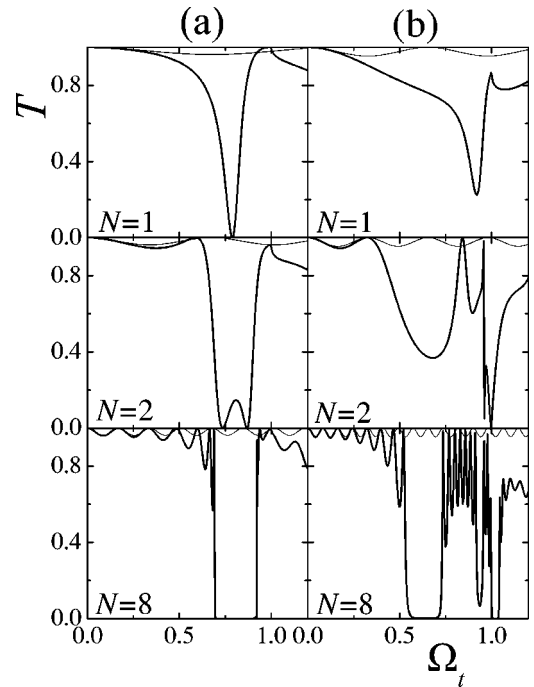


FIG. 4. Transmittance for a longitudinal (a) and a transverse (b) elastic wave incident normally on a slab of  $N$  layers of a fcc crystal ( $a = 3.72$  mm), parallel to the (001) surface, of steel spheres ( $S = 0.585$  mm) in an infinite, nonabsorbing polyester matrix. The thin lines show the results of the effective-medium approximation.

our analysis of the physics of this dip, we can assume that the host medium of polyester extends to infinity and that it is not absorbing.

### III. PHYSICAL ORIGIN OF THE DIPS IN THE TRANSMISSION SPECTRA

We believe that the physical reason for the observed dips in the transmission spectra results from the multiple scattering between the spheres of the plane, and is more akin to the way hybridization gaps open up in a bulk crystal. To begin with, we calculate (thick lines in Figs. 4) the transmittance  $T$  of a plane elastic wave (longitudinal or transverse) incident normally on a slab consisting of  $N = 1, 2, 8$  planes of steel spheres of radius  $S = 0.585$  mm. The planes are arranged relative to each other as successive (001) planes of a fcc crystal of lattice constant  $a = \sqrt{2}a_0 = 3.72$  mm. In all cases the host medium which extends to infinity on either side of the slab is nonabsorbing polyester. In the same figures we show by thin lines the transmittance for an effective homogeneous slab, of the appropriate thickness  $D = Na/2$ , in polyester, using the effective-medium approximation of Gaunard and Wertman<sup>13</sup> in the long wavelength limit ( $\omega \rightarrow 0$ ). The effective-medium results show quite clearly the Fabry-Perot-type oscillations; one can see that the period of these oscillations is inversely proportional to the thickness of the slab. But the effective-medium approximation does not reproduce the observed dips we are interested in.

One can see that the dips in the transmittance of the one-plane structure develop into practically forbidden gaps (the

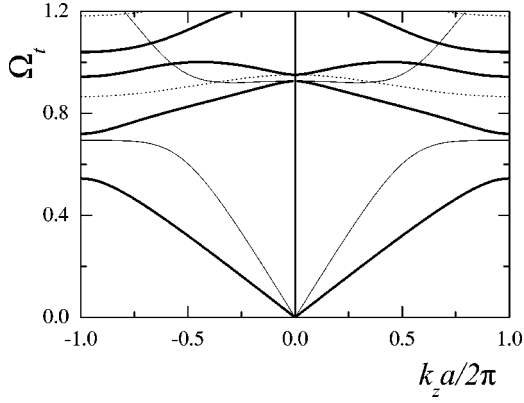


FIG. 5. The phononic frequency band structure normal to the (001) surface of a fcc crystal ( $a=3.72$  mm) of steel spheres ( $S=0.585$  mm) in nonabsorbing polyester. The thin (thick) solid lines refer to longitudinal (transverse) bands and the dotted lines refer to deaf bands.

elastic wave does not penetrate the slab) as the number of planes increases. To make the point clearer we present in Fig. 5 the frequency band structure normal to the (001) surface for the (infinite) fcc crystal of steel spheres in nonabsorbing polyester. The thin solid lines in Fig. 5 denote longitudinal bands, while the thick solid lines are transverse bands, and will couple with, respectively, longitudinal and transverse elastic waves incident normally on a (001) slab of the material. The dotted lines are deaf bands which practically do not couple with elastic waves incident normally on the slab (for a clarification of what is meant by longitudinal, transverse, and deaf bands in phononic crystals see Sec. VII of Ref. 2).

Looking at the transmittance of transverse waves [Figs. 4(b)] we can readily see that the lower frequency dip, which appears in the transmission spectra of slabs two and eight layers thick about  $\Omega_t=0.68$ , corresponds to a Bragg gap opening up, about the same frequency, between the first and second transverse bands of Fig. 5. We note that a similar gap for longitudinal waves appears at much higher frequencies (outside the region considered in Figs. 4) and, therefore, one does not see the corresponding dip in the transmittance of longitudinal waves in Fig. 4(a).

The dips in the transmittance of longitudinal and transverse waves through the monolayer of steel spheres (Fig. 4,  $N=1$ ) correspond to hybridization-induced gaps in the frequency bands of these waves opening up about the frequency positions of the above dips, as shown in Fig. 5. The hybridization-induced gap in the longitudinal bands is perhaps easier to explain. We have established<sup>14,16</sup> that when a single plane of steel spheres is placed in polyester there exists, at  $\Omega_t=0.81$ , a virtual bound state (a resonant state of finite lifetime) of the longitudinal displacement field, for  $\mathbf{k}_{\parallel}=\mathbf{0}$ , which peaks about the said plane but falls to a much lower value away from it. Therefore, virtual bound states on neighbor planes of spheres will couple weakly with each other, resulting in a relatively flat band as shown schematically in Fig. 6 (we always assume that  $\mathbf{k}_{\parallel}=\mathbf{0}$ ). On the same figure we also show the band corresponding to the longitudinal displacement field in the homogeneous effective medium that one would obtain in the absence of interaction with

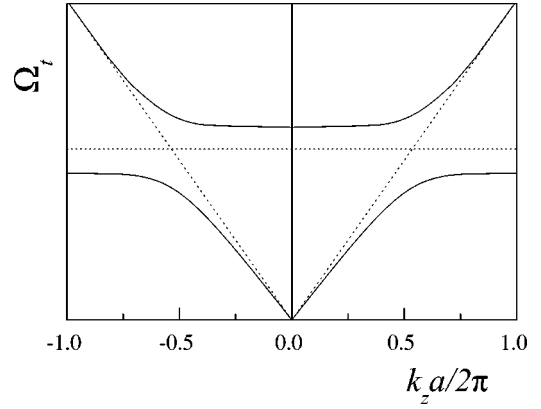


FIG. 6. Schematic representation of a hybridization-induced gap. The solid (dotted) lines show the hybridized (unhybridized) bands.

the above flat band. Because an interaction between them does exist, they hybridize and we obtain the bands represented by the solid lines in Fig. 6, which are similar to the actual bands (thin solid lines in Fig. 5). Naturally the modes at the top of the lower band (below the gap) and those at the bottom of the higher band (above the gap) are hybridized modes in the above sense. An incident longitudinal wave excites these bands, leading to finite transmission through a finite slab of the material, as shown in Fig. 4(a). By the same token, the hybridization-induced gap is responsible for the dips in the transmission spectra at the corresponding frequencies [see Fig. 4(a)]. That the mechanism we have described is effective even for a single plane of spheres, should not surprise; in the present case, it is the interaction between the virtual bound state on the single plane and the propagating modes in the host effective medium which determines the physics of the situation. As the coverage increases, the stronger interaction between the spheres results in virtual bound states on the plane of larger frequency width (shorter lifetime) which, in turn, leads to more effective hybridization with the host medium and hence to more pronounced dips in the transmission spectra [see Figs. 1(c),1(d)].

One can interpret the transverse bands of Fig. 5 as a result of hybridization between a wide band corresponding to propagation in an effective host medium and more than one relatively narrow bands originating from virtual bound states on the planes of spheres, in a manner similar to that we have described for the longitudinal bands. The detailed structure of the shown hybridized bands is more complicated because of the greater number of unhybridized bands involved. We shall not be concerned with a detailed analysis of the transverse bands, especially since they are not directly relevant to the experimental data. Whatever the physical interpretation of the origin of these bands, they are consistent with the transmission spectra of Fig. 4(b); for example, the gap about  $\Omega_t=0.94$  in Fig. 5 leads to the observed dip in the transmittance about the same frequency in Fig. 4(b).

Phenomena analogous to the ones described here, which can be interpreted on the basis of hybridization between states localized on planes of spheres and extended states in an effective host medium, have also been discussed in rela-

tion to metallodielectric photonic crystals.<sup>15</sup> Another feature, common to both situations, is the crowding of the Fabry-Perot-type oscillations in the vicinity of the gap, shown clearly in Figs. 4(a), 4(b) for  $N=8$ , which is due to the flattening of the bands near the edges of the gap.<sup>15</sup>

### ACKNOWLEDGMENTS

This work has been supported by the Institute of Communication and Computer Systems (ICCS) of the National Technical University of Athens. Partial support from the University of Athens is also acknowledged. R. Sainidou was supported by the State Foundation (IKY) of Greece.

### APPENDIX

In this appendix we derive explicit expressions for the transmission and reflection matrices which describe the scattering of an elastic plane wave, of angular frequency  $\omega$ , incident on a homogeneous and isotropic plate, of thickness  $d$ , sandwiched between two semi-infinite homogeneous and isotropic media. Though similar expressions can be found in the literature, we thought it necessary to include this appendix to provide the formulas in a form compatible to the formalism we have developed in Ref. 2. The plate is normal to the  $z$  axis, the direction of which (left to right) is specified by the unit vector  $\hat{\mathbf{e}}_z$ . The elastic properties of the different media  $j$  ( $j=1,2,3$  from left to right), are characterized by the mass densities  $\rho_j$  and the longitudinal and transverse propagation velocities  $c_{\nu j}$ , where  $\nu=l$  and  $t$ , respectively. We note that the final expressions for the transmission and reflection matrices, given below, remain valid when  $d=0$ , in which case they describe the transmission and reflection at an interface between the two semi-infinite media ( $j=1$  and  $j=3$ ). In this case, the actual values of the elastic constants of the plate ( $j=2$ ) are irrelevant.

Taking advantage of the translation invariance parallel to the interfaces, at  $z=0$  and  $z=d$ , we write the wave vector of a plane wave in medium  $j$  as  $\mathbf{q}_{\nu j}^{\pm} = \mathbf{q}_{\parallel}^{\pm} [(\omega/c_{\nu j})^2 - \mathbf{q}_{\parallel}^2]^{1/2} \hat{\mathbf{e}}_z$ , where  $\mathbf{q}_{\parallel}$  is the component of the wave vector parallel to the interfaces and the  $+$  ( $-$ ) sign denotes propagation to the positive (negative)  $z$  direction. We refer the waves on the left side of the plate to an origin  $\mathbf{A}_+ = (0,0,0)$  and the waves on the right side of the plate to an origin  $\mathbf{A}_- = (0,0,d)$ .

We assume, to begin with, that all three media are solid, and write the displacement vector associated with a plane elastic wave (it can be longitudinal or transverse) incident on the plate, as follows:

$$\mathbf{u}_{in}^{s'}(\mathbf{r}) = \sum_{i'=1}^3 [u_{in}]_{i'}^{s'} \exp[i\mathbf{q}_{\nu j}^{s'} \cdot (\mathbf{r} - \mathbf{A}_{s'})] \hat{\mathbf{e}}_{i'}, \quad (\text{A1})$$

where  $s' = +(-)$  corresponds to a wave incident from the left (right). We note that a longitudinal incident wave ( $\nu' = l$ ) has only one component,  $i' = 1$ , and then  $\hat{\mathbf{e}}_1$  denotes the radial unit vector along the direction of  $\mathbf{q}_{l j}^{s'}$ ; for  $\nu' = t$  the nonzero components of the incident wave are two,  $i' = 2$  or 3

( $p$  or  $s$  polarized wave), and then  $\hat{\mathbf{e}}_2, \hat{\mathbf{e}}_3$  denote the polar and azimuthal unit vectors, respectively, which are orthogonal to  $\mathbf{q}_{t j}^{s'}$ . We can now write the corresponding transmitted and reflected waves in the form

$$\mathbf{u}_{tr}^{s'}(\mathbf{r}) = \sum_{i=1}^3 [u_{tr}]_i^{s'} \exp[i\mathbf{q}_{\nu j}^{s'} \cdot (\mathbf{r} - \mathbf{A}_{-s'})] \hat{\mathbf{e}}_i \quad (\text{A2})$$

and

$$\mathbf{u}_{rf}^{-s'}(\mathbf{r}) = \sum_{i=1}^3 [u_{rf}]_i^{-s'} \exp[i\mathbf{q}_{\nu j}^{-s'} \cdot (\mathbf{r} - \mathbf{A}_{s'})] \hat{\mathbf{e}}_i, \quad (\text{A3})$$

respectively. The amplitudes of the transmitted and reflected waves are related to that of the incident wave through the equations

$$\begin{aligned} [u_{tr}]_i^{s'} &= \sum_{i'=1}^3 N_{ii'}^{s' s'} [u_{in}]_{i'}^{s'}, \\ [u_{rf}]_i^{-s'} &= \sum_{i'=1}^3 N_{ii'}^{-s' s'} [u_{in}]_{i'}^{s'}. \end{aligned} \quad (\text{A4})$$

Allowing for multiple reflections at the interfaces, one can show that the matrices  $\mathbf{N}^{s' s'}$  which describe the transmission through and the reflection by the plate can be written in the following form:

$$\mathbf{N}^{++} = \mathbf{T}^{(2,3)} [\mathbf{I} - \mathbf{P}\mathbf{R}^{(2,1)}\mathbf{P}\mathbf{R}^{(2,3)}]^{-1} \mathbf{P}\mathbf{T}^{(1,2)},$$

$$\mathbf{N}^{+-} = \mathbf{R}^{(3,2)} + \mathbf{T}^{(2,3)}\mathbf{P}\mathbf{R}^{(2,1)} [\mathbf{I} - \mathbf{P}\mathbf{R}^{(2,3)}\mathbf{P}\mathbf{R}^{(2,1)}]^{-1} \mathbf{P}\mathbf{T}^{(3,2)},$$

$$\mathbf{N}^{-+} = \mathbf{R}^{(1,2)} + \mathbf{T}^{(2,1)}\mathbf{P}\mathbf{R}^{(2,3)} [\mathbf{I} - \mathbf{P}\mathbf{R}^{(2,1)}\mathbf{P}\mathbf{R}^{(2,3)}]^{-1} \mathbf{P}\mathbf{T}^{(1,2)},$$

$$\mathbf{N}^{--} = \mathbf{T}^{(2,1)} [\mathbf{I} - \mathbf{P}\mathbf{R}^{(2,3)}\mathbf{P}\mathbf{R}^{(2,1)}]^{-1} \mathbf{P}\mathbf{T}^{(3,2)}, \quad (\text{A5})$$

where  $\mathbf{I}$  is the  $3 \times 3$  unit matrix and  $\mathbf{P}$  is a diagonal matrix, with elements  $P_{11} = \exp(i|q_{12z}|d)$ ,  $P_{22} = P_{33} = \exp(i|q_{t2z}|d)$ , which describes the propagation of a plane wave in the plate. The  $3 \times 3$  matrices  $\mathbf{T}^{(j,j')}$  and  $\mathbf{R}^{(j,j')}$  describe the transmission and reflection of an elastic plane wave incident from medium  $j$  on the interface between media  $j$  and  $j'$ ; they are obtained by imposing the boundary conditions of continuity of the displacement vector and of the surface traction at the interface. For  $(j,j') = (1,2), (2,3)$  (incidence from the left) the nonzero elements of these matrices are found by solving the following three systems of linear equations:

$$\begin{pmatrix} -\sin \theta_{lj} & \cos \theta_{lj} & \sin \theta_{lj'} & \cos \theta_{lj'} \\ \cos \theta_{lj} & \sin \theta_{lj} & \cos \theta_{lj'} & -\sin \theta_{lj'} \\ \sin 2\theta_{lj} & -\frac{c_{lj}}{c_{lj}} \cos 2\theta_{lj} & \frac{\rho_{j'}}{\rho_j} \left( \frac{c_{lj'}}{c_{lj}} \right)^2 \frac{c_{lj}}{c_{lj'}} \sin 2\theta_{lj'} & \frac{\rho_{j'}}{\rho_j} \frac{c_{lj'}}{c_{lj}} \frac{c_{lj}}{c_{lj'}} \cos 2\theta_{lj'} \\ \cos 2\theta_{lj} & \frac{c_{lj}}{c_{lj}} \sin 2\theta_{lj} & -\frac{\rho_{j'}}{\rho_j} \frac{c_{lj'}}{c_{lj}} \cos 2\theta_{lj'} & \frac{\rho_{j'}}{\rho_j} \frac{c_{lj'}}{c_{lj}} \sin 2\theta_{lj'} \end{pmatrix} \begin{pmatrix} R_{11}^{(j,j')} \\ R_{21}^{(j,j')} \\ T_{11}^{(j,j')} \\ T_{21}^{(j,j')} \end{pmatrix} = \begin{pmatrix} \sin \theta_{lj} \\ \cos \theta_{lj} \\ \sin 2\theta_{lj} \\ -\cos 2\theta_{lj} \end{pmatrix}, \quad (\text{A6})$$

$$\begin{pmatrix} \sin \theta_{lj} & \cos \theta_{lj} & -\sin \theta_{lj'} & \cos \theta_{lj'} \\ \cos \theta_{lj} & -\sin \theta_{lj} & \cos \theta_{lj'} & \sin \theta_{lj'} \\ \sin 2\theta_{lj} & \frac{c_{lj}}{c_{lj}} \cos 2\theta_{lj} & \frac{\rho_{j'}}{\rho_j} \frac{c_{lj'}}{c_{lj}} \sin 2\theta_{lj'} & -\frac{\rho_{j'}}{\rho_j} \frac{c_{lj'}}{c_{lj}} \cos 2\theta_{lj'} \\ -\cos 2\theta_{lj} & \frac{c_{lj}}{c_{lj}} \sin 2\theta_{lj} & \frac{\rho_{j'}}{\rho_j} \frac{c_{lj'}}{c_{lj}} \cos 2\theta_{lj'} & \frac{\rho_{j'}}{\rho_j} \frac{c_{lj'}}{c_{lj}} \sin 2\theta_{lj'} \end{pmatrix} \begin{pmatrix} R_{22}^{(j,j')} \\ R_{12}^{(j,j')} \\ T_{22}^{(j,j')} \\ T_{12}^{(j,j')} \end{pmatrix} = \begin{pmatrix} -\sin \theta_{lj} \\ \cos \theta_{lj} \\ \sin 2\theta_{lj} \\ \cos 2\theta_{lj} \end{pmatrix}, \quad (\text{A7})$$

$$\begin{pmatrix} 1 & -1 \\ \cos \theta_{lj} & \frac{\rho_{j'}}{\rho_j} \frac{c_{lj'}}{c_{lj}} \cos \theta_{lj'} \end{pmatrix} \begin{pmatrix} R_{33}^{(j,j')} \\ T_{33}^{(j,j')} \end{pmatrix} = \begin{pmatrix} -1 \\ \cos \theta_{lj} \end{pmatrix}, \quad (\text{A8})$$

where  $\sin \theta_{vj} = |\mathbf{q}_{\parallel}| c_{vj} / \omega$ ,  $\cos \theta_{vj} = + (1 - \sin^2 \theta_{vj})^{1/2}$ . For  $(j, j') = (2, 1), (3, 2)$  (incidence from the right) the corresponding transmission and reflection matrices are also determined by Eqs. (A6)–(A8) with the difference that the non-diagonal elements of  $\mathbf{T}^{(j,j')}$  and  $\mathbf{R}^{(j,j')}$  appear in these equations with the opposite sign.

If one, or more, of the media under consideration are fluid, where transverse waves cannot exist, the nonzero elements of  $\mathbf{T}^{(j,j')}$  and  $\mathbf{R}^{(j,j')}$  entering Eq. (A5) are evaluated by imposing the boundary conditions at the interfaces appropriate in this case. In this way, instead of Eqs. (A6)–(A8), we obtain

$$\begin{pmatrix} \cos \theta_{lj} & \sin \theta_{lj} & \cos \theta_{lj'} \\ \sin 2\theta_{lj} & -\frac{c_{lj}}{c_{lj}} \cos 2\theta_{lj} & 0 \\ \cos 2\theta_{lj} & \frac{c_{lj}}{c_{lj}} \sin 2\theta_{lj} & -\frac{\rho_{j'}}{\rho_j} \frac{c_{lj'}}{c_{lj}} \end{pmatrix} \begin{pmatrix} R_{11}^{(j,j')} \\ R_{21}^{(j,j')} \\ T_{11}^{(j,j')} \end{pmatrix} = \begin{pmatrix} \cos \theta_{lj} \\ \sin 2\theta_{lj} \\ -\cos 2\theta_{lj} \end{pmatrix}, \quad (\text{A9})$$

$$\begin{pmatrix} \sin \theta_{lj} & \cos \theta_{lj} & \cos \theta_{lj'} \\ -\cos 2\theta_{lj} & \frac{c_{lj}}{c_{lj}} \sin 2\theta_{lj} & 0 \\ \sin 2\theta_{lj} & \frac{c_{lj}}{c_{lj}} \cos 2\theta_{lj} & -\frac{\rho_{j'}}{\rho_j} \frac{c_{lj'}}{c_{lj}} \end{pmatrix} \begin{pmatrix} R_{22}^{(j,j')} \\ R_{12}^{(j,j')} \\ T_{12}^{(j,j')} \end{pmatrix} = \begin{pmatrix} -\sin \theta_{lj} \\ \cos 2\theta_{lj} \\ \sin 2\theta_{lj} \end{pmatrix}, \quad (\text{A10})$$

$$R_{33}^{(j,j')} = 1 \quad (\text{A11})$$

for an interface between a solid (left) and a fluid (right) medium;

$$\begin{pmatrix} \cos \theta_{lj} & \cos \theta_{lj'} & -\sin \theta_{lj'} \\ -1 & \frac{\rho_{j'}}{\rho_j} \frac{c_{lj'}}{c_{lj}} \cos 2\theta_{lj'} & -\frac{\rho_{j'}}{\rho_j} \frac{c_{lj'}}{c_{lj}} \sin 2\theta_{lj'} \\ 0 & \frac{c_{lj'}}{c_{lj'}} \sin 2\theta_{lj'} & \cos 2\theta_{lj'} \end{pmatrix} \times \begin{pmatrix} R_{11}^{(j,j')} \\ T_{11}^{(j,j')} \\ T_{21}^{(j,j')} \end{pmatrix} = \begin{pmatrix} \cos \theta_{lj} \\ 1 \\ 0 \end{pmatrix} \quad (\text{A12})$$

for an interface between a fluid (left) and a solid (right) medium, and

$$\begin{pmatrix} \cos \theta_{lj} & \cos \theta_{lj'} \\ \sin \theta_{lj} & -\frac{\rho_{j'}}{\rho_j} \sin \theta_{lj'} \end{pmatrix} \begin{pmatrix} R_{11}^{(j,j')} \\ T_{11}^{(j,j')} \end{pmatrix} = \begin{pmatrix} \cos \theta_{lj} \\ -\sin \theta_{lj} \end{pmatrix} \quad (\text{A13})$$

for an interface between two fluid media.

Since our method of calculation<sup>2</sup> is meant to deal with composite layered structures of phononic crystals, where a plate or an interface constitutes a component of a unit slice which in general contains, in addition, planes of spheres of given 2D periodicity, it is convenient to write the parallel component of the wave vector in the form  $\mathbf{q}_{\parallel} = \mathbf{k}_{\parallel} + \mathbf{g}$ , where  $\mathbf{g}$  is a certain reciprocal vector, and then express the waves on the left (right) of the plate with respect to an origin

$-\mathbf{dl}(\mathbf{dr})$  from  $\mathbf{A}_+(\mathbf{A}_-)$ . Referred to these origins the transmission and reflection matrix elements of the homogeneous plate become

$$\begin{aligned} Q_{\mathbf{g}i;\mathbf{g}'i'}^{\text{I}} &= \delta_{\mathbf{g}\mathbf{g}'} N_{ii'}^{++} \exp[i(\mathbf{K}_{\mathbf{g}\nu;3}^+ \cdot \mathbf{d}_r + \mathbf{K}_{\mathbf{g}'\nu';1}^+ \cdot \mathbf{d}_l)], \\ Q_{\mathbf{g}i;\mathbf{g}'i'}^{\text{II}} &= \delta_{\mathbf{g}\mathbf{g}'} N_{ii'}^{+-} \exp[i(\mathbf{K}_{\mathbf{g}\nu;3}^+ \cdot \mathbf{d}_r - \mathbf{K}_{\mathbf{g}'\nu';3}^- \cdot \mathbf{d}_r)], \\ Q_{\mathbf{g}i;\mathbf{g}'i'}^{\text{III}} &= \delta_{\mathbf{g}\mathbf{g}'} N_{ii'}^{-+} \exp[-i(\mathbf{K}_{\mathbf{g}\nu;1}^- \cdot \mathbf{d}_l - \mathbf{K}_{\mathbf{g}'\nu';1}^+ \cdot \mathbf{d}_l)], \\ Q_{\mathbf{g}i;\mathbf{g}'i'}^{\text{IV}} &= \delta_{\mathbf{g}\mathbf{g}'} N_{ii'}^{--} \exp[-i(\mathbf{K}_{\mathbf{g}\nu;1}^- \cdot \mathbf{d}_l + \mathbf{K}_{\mathbf{g}'\nu';3}^- \cdot \mathbf{d}_r)], \end{aligned} \quad (\text{A14})$$

where  $\mathbf{K}_{\mathbf{g}\nu;j}^{\pm} = \mathbf{k}_{\parallel} + \mathbf{g}^{\pm} [(\omega/c_{\nu j})^2 - (\mathbf{k}_{\parallel} + \mathbf{g})^2]^{1/2} \hat{\mathbf{e}}_z$ .

\*Also at Section of Solid State Physics, University of Athens, Panepistimioupolis GR-157 84, Athens, Greece.

<sup>1</sup> *Photonic Crystals and Light Localization in the 21<sup>st</sup> Century*, edited by C.M. Soukoulis (Kluwer Academic, Dordrecht, 2001).

<sup>2</sup> I.E. Psarobas, N. Stefanou, and A. Modinos, Phys. Rev. B **62**, 278 (2000).

<sup>3</sup> I.E. Psarobas, N. Stefanou, and A. Modinos, Phys. Rev. B **62**, 5536 (2000).

<sup>4</sup> I.E. Psarobas, Phys. Rev. B **64**, 012303 (2001).

<sup>5</sup> I.E. Psarobas, A. Modinos, R. Sainidou, and N. Stefanou, Phys. Rev. B **65**, 064307 (2002).

<sup>6</sup> V.K. Kinra, N.A. Day, K. Maslov, B.K. Henderson, and G. Diderich, J. Mech. Phys. Solids **46**, 153 (1998).

<sup>7</sup> K. Maslov, V.K. Kinra, and B.K. Henderson, Mech. Mater. **31**, 175 (1999).

<sup>8</sup> V.K. Kinra, B.K. Henderson, and K. Maslov, J. Mech. Phys. Solids **47**, 2147 (1999).

<sup>9</sup> K. Maslov, V.K. Kinra, and B.K. Henderson, Mech. Mater. **32**, 175 (2000).

<sup>10</sup> A.G. Every, R.E. Vines, and J.P. Wolfe, Ultrasonics **38**, 761 (2000).

<sup>11</sup> R.W. Wood, Philos. Mag. **4**, 396 (1902).

<sup>12</sup> M. Inoue, K. Ohtaka, and S. Yanagawa, Phys. Rev. B **25**, 689 (1982).

<sup>13</sup> G.C. Gaunaurd and W. Wertman, J. Acoust. Soc. Am. **85**, 541 (1989).

<sup>14</sup> We obtain  $\Delta n(\omega; \mathbf{k}_{\parallel})$ , the difference between the density of modes of the elastic field in the system consisting of a layer of spheres in a host medium and that of the elastic field in the host medium, using the relation between  $\Delta n$  and the scattering ( $S$ ) matrix for the plane of spheres, as given by Ohtaka *et al.* (Ref. 16).

<sup>15</sup> V. Yannopoulos, A. Modinos, and N. Stefanou, Phys. Rev. B **60**, 5359 (1999).

<sup>16</sup> K. Ohtaka, Y. Suda, S. Nagano, T. Ueta, A. Imada, T. Koda, J.S. Bae, K. Mizuno, S. Yano, and Y. Segawa, Phys. Rev. B **61**, 5267 (2000).